EXTENDED PDF FORMAT
SPONSORED BY

BIO-RAD

http://discover.bio-rad.com

Synthesis of Ultra-Incompressible Superhard Rhenium Diboride at Ambient Pressure

Hsiu-Ying Chung, *et al.*

Science **316**, 436 (2007);
DOI: 10.1126/science.1139322

The following resources related to this article are available online at www.sciencemag.org (this information is current as of June 11, 2007):

Updated information and services, including high-resolution figures, can be found in the online version of this article at:
http://www.sciencemag.org/cgi/content/full/316/5823/436

Supporting Online Material can be found at:
http://www.sciencemag.org/cgi/content/full/316/5823/436/DC1

This article **cites 26 articles**, 1 of which can be accessed for free:
http://www.sciencemag.org/cgi/content/full/316/5823/436#otherarticles

This article appears in the following **subject collections**:
Materials Science
http://www.sciencemag.org/cgi/collection/mat_sci

Information about obtaining **reprints** of this article or about obtaining **permission to reproduce this article** in whole or in part can be found at:
http://www.sciencemag.org/about/permissions.dtl

Downloaded from www.sciencemag.org on June 11, 2007

Science (print ISSN 0036-8075; online ISSN 1095-9203) is published weekly, except the last week in December, by the American Association for the Advancement of Science, 1200 New York Avenue NW, Washington, DC 20005. Copyright c 2007 by the American Association for the Advancement of Science; all rights reserved. The title SCIENCE is a registered trademark of AAAS.

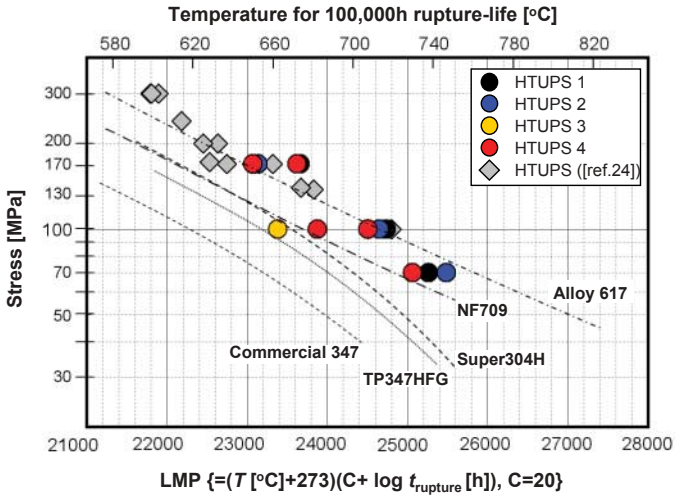

Fig. 5. Larson Miller Parameter (LMP) of HTUPS series plotted as a function of stress, together with those of some benchmark commercial high-temperature austenitic stainless steels and the Ni-base alloy 617 (*24*–*26*). The LMP scales with both creep-rupture time and test temperature.

indicated amenability to joining by conventional welding techniques, which is a key requirement for many applications.

The finding that low amounts of Al are sufficient to form Al_2O_3 scales on stable fcc austenitic stainless steels if Ti and V additions are eliminated (or minimized) also holds great promise for modifying other existing families of high-temperature alloys for Al_2O_3 scale formation, not just the HTUPS family. Creep-resistant, Al_2O_3-forming austenitic stainless steels will enable higher operating temperatures and greater durability in a range of energy-conversion system applications, as well as in the chemical and process industries.

References and Notes

1. R. Viswanathan, W. Bakker, *J. Mat. Eng. Per.* **10**, 81 (2001).
2. R. Viswanathan, W. Bakker, *J. Mat. Eng. Per.* **10**, 96 (2001).
3. T. Sourmail, *Mat. Sci. Technol.* **17**, 1 (2001).
4. M. Taneike, F. Abe, K. Sawada, *Nature* **424**, 294 (2003).
5. P. Kofstad, Ed., *High Temperature Corrosion* (Elsevier, London, 1988).
6. E. J. Opila, *Mater. Sci. Forum* **461-464**, 765 (2004).
7. B. A. Pint, R. Peraldi, P. J. Maziasz, *Mater. Sci. Forum* **461-464**, 815 (2004).
8. V. Ramakrishnan, J. A. McGurty, N. Jayaraman, *Oxid. Met.* **30**, 185 (1988).
9. D. Satyanarayana, G. Malakondaiah, D. Sarma, *Mater. Sci. Eng. A* **323**, 119 (2002).
10. T. Fujioka, M. Kinugasa, S. Iizumi, S. Teshima, I. Shimizu, U.S. Patent 3,989,514 (1976).
11. J. A. McGurty, U.S. Patent 4,086,085 (1978).
12. J. C. Pivin *et al.*, *Corros. Sci.* **20**, 351 (1980).
13. N. V. Bangaru, R. C. Krutenat, *J. Vac. Sci. B* **2**, 806 (1984).
14. Y. Zhang *et al.*, *Surf. Coat. Technol.* **188-189**, 35 (2004).
15. P. J. Maziasz, *J. Met.* **41**, 14 (1989).
16. M. P. Brady, C. T. Liu, Y. Yamamoto, Z. P. Lu, H. Meyer, "Multi-Phase High Temperature Alloys: Exploration of Laves Phase Strengthening of Steels," Proceedings of the 19th Annual Conference on Fossil Energy Materials, Knoxville, TN, 9 to 11 May 2005; available at www.ornl.gov/sci/fossil/.
17. Y. Yamamoto, Z. P. Lu, M. P. Brady, C. T. Liu, P. F. Tortorelli, "Multi-Phase High Temperature Alloys: Exploration of Laves Phase Strengthening of Steels," Proceedings of the 20th Annual Conference on Fossil Energy Materials, Knoxville, TN, 12 to 14 June 2006; available at www.ornl.gov/sci/fossil/.
18. I. Kvernes, M. Oliverire, P. Kofstad, *Corros. Sci.* **17**, 237 (1977).
19. M. P. Brady *et al.*, "Oxidation Resistant, High Creep Strength Austenitic Stainless Steel," U.S. Patent Disclosure (4 January 2007).
20. C. Wagner, *Z. Elektrochem.* **63**, 772 (1959).
21. J. P. Shingledecker, P. J. Maziasz, N. D. Evans, M. J. Pollard, in *Creep Deformation and Fracture, Design, and Life Extension*, R. S. Mishra, J. C. Earthman, S. V. Raj, R. Viswanathan, Eds. (TMS, Warrendale, PA), pp. 129–138.
22. B. A. Pint, *J. Eng. Gas Turbines Power* **128**, 370 (2006).
23. D. J. Young, B. A. Pint, *Oxid. Met.* **66**, 3/4, 137 (2006).
24. R. W. Swindeman, P. J. Maziasz, E. Bolling, J. F. King, "Evolution of advanced austenitic alloys relative to alloy design criteria for steam service: Part 1–Lean stainless steels" (Oak Ridge National Laboratory Rep. ORNL-6629/P1, Oak Ridge, TN, 1990).
25. J. P. Shingledecker, P. J. Maziasz, N. D. Evans, M. J. Pollard, in *Creep and Fracture in High Temperature Components—Design and Life Assessment Issues* (Destech, Lancaster, PA, 2005), pp. 99–109.
26. Allegheny Ludlum, *Technical Data Blue Sheet, Stainless Steels, types 321, 347 and 348* (ATI Allegheny Ludlum Corp., Pittsburgh, PA, 2003); www.alleghenyludlum.com.

27. We thank J. Shingledecker, P. Tortorelli, and E. George for helpful comments on this manuscript. This work was funded by the U.S. Department of Energy (DOE), Fossil Energy Advanced Research Materials Program. Additional funding and collaboration with the U.S. DOE Distributed Energy Program and the Division of Materials Sciences and Engineering, Office of Basic Energy Sciences, are also acknowledged. The SHaRE User Facility at Oak Ridge National Laboratory, sponsored by the U.S. DOE, Office of Basic Energy Sciences, Division of Scientific User Facilities, is also acknowledged. Oak Ridge National Laboratory is managed by UT-Battelle, LLC, for the U.S. DOE under contract DE-AC05-00OR22725.

17 November 2006; accepted 1 March 2007
10.1126/science.1137711

Synthesis of Ultra-Incompressible Superhard Rhenium Diboride at Ambient Pressure

Hsiu-Ying Chung,[1,2]* Michelle B. Weinberger,[1]* Jonathan B. Levine,[1] Abby Kavner,[3] Jenn-Ming Yang,[2] Sarah H. Tolbert,[1]† Richard B. Kaner[1,2]†

The quest to create superhard materials rarely strays from the use of high-pressure synthetic methods, which typically require gigapascals of applied pressure. We report that rhenium diboride (ReB_2), synthesized in bulk quantities via arc-melting under ambient pressure, rivals materials produced with high-pressure methods. Microindentation measurements on ReB_2 indicated an average hardness of 48 gigapascals under an applied load of 0.49 newton, and scratch marks left on a diamond surface confirmed its superhard nature. Its incompressibility along the *c* axis was equal in magnitude to the linear incompressibility of diamond. In situ high-pressure x-ray diffraction measurements yielded a bulk modulus of 360 gigapascals, and radial diffraction indicated that ReB_2 is able to support a remarkably high differential stress. This combination of properties suggests that this material may find applications in cutting when the formation of carbides prevents the use of traditional materials such as diamond.

The design of superhard materials is motivated by a need for robust, chemically diverse compounds for industrial applications ranging from abrasives and cutting tools to scratch-resistant coatings. Although diamond, with the highest known hardness (70 to 100 GPa), has traditionally been used to fulfill many of these needs, there are limits to its applicability. For example, diamond is not used to cut steel and other ferrous metals because of the detrimental formation of iron carbide during high-speed machining. Therefore, there is a need for synthetic materials that can be used in place of diamond. Cubic boron nitride (BN), the second hardest material (45 to 50 GPa), is used to cut steel because iron borides and nitrides are much less stable. However, cubic BN must be synthesized under extreme pressures (>5 GPa) and temperatures (>1500°C), making it expensive (*1*). Two other compounds that have been synthesized recently, B_6O (*2*) and cubic BC_2N

[1]Department of Chemistry and Biochemistry and the California NanoSystems Institute, University of California, Los Angeles, CA 90095–1569, USA. [2]Department of Materials Science and Engineering, University of California, Los Angeles, CA 90095–1595, USA. [3]Department of Earth and Space Sciences, University of California, Los Angeles, CA 90095-1567, USA.

*These authors contributed equally to this work.
†To whom correspondence should be addressed. E-mail: tolbert@chem.ucla.edu (S.H.T.); kaner@chem.ucla.edu (R.B.K.)

Downloaded from www.sciencemag.org on June 11, 2007

(*3*), rival the hardness of cubic BN. However, their syntheses also require extreme pressures, exceeding 5 GPa for B_6O and 18 GPa for BC_2N.

Our approach to creating ultra-incompressible superhard materials has been to optimize two design parameters: high valence-electron density and bond covalency (*4*, *5*). High electron densities can be found among the later transition metals, whereas small first-row main-group elements, such as B, C, and N, form the strongest covalent bonds (*6*). Among the transition metals, Os has the highest valence-electron density (0.572 electrons/Å^3) and a reported bulk modulus between 395 and 462 GPa (*7*–*9*) that rivals that of diamond (442 GPa) (*10*, *11*). However, unlike diamond, the hardness of Os metal is only 4 GPa. This can be explained by the nondirectional metallic bonding in Os versus the short, highly covalent, directional bonds formed by sp^3 hybridized C atoms in diamond. The strength and directionality of covalent bonds limit the creation and propagation of defects, which in turn causes diamond to resist plastic deformation, resulting in diamond's exceptional hardness. By optimizing covalent bonding and valence-electron density, we recently succeeded in designing, synthesizing, and characterizing an ultra-incompressible hard material, OsB_2 (*4*). In searching for even harder materials, we looked closely at the elements surrounding Os in the periodic table. Re, which lies directly to the left of Os, has a slightly lower valence-electron density (0.4761 electrons/Å^3) that produces a similar bulk modulus of 360 GPa (*12*). Despite being highly incompressible, the hardness of Re metal is also low, between 1.3 and 3.2 GPa, because of its delocalized nondirectional metallic bonding (*13*, *14*). Incorporating B into the interstitial sites of Re to form ReB_2 requires only a 5% expansion of the Re lattice. This results in the shortest metal-metal bonds of any known transition-metal diboride (*15*). In contrast, the Os lattice expands by approximately 10% upon the incorporation of B atoms to form OsB_2 and undergoes a distortion to an orthorhombic phase. Applying our design criteria, ReB_2 is thus considered to be the most likely candidate for improving on the mechanical properties of OsB_2.

ReB_2 has the highest B:Re ratio among the known Re_xB_y phases—Re_3B, Re_7B_3, and ReB_2 (*16*)—and therefore contains the greatest degree of covalent bonding. The structure of ReB_2 consists of alternating layers of hexagonal close-packed Re and puckered hexagonal networks of B (Fig. 1). The result is a compound that is layered perpendicular to the *c* axis along the (00*l*) planes. Recent theoretical calculations have shown that there are strong covalent B-B and Os-B bonds in OsB_2 (*17*–*20*). By analogy, ReB_2 should contain similar covalent B-B and Re-B bonds, with the Re-B bonds in ReB_2 expected to be shorter and stronger than those in OsB_2 because of the minimal lattice expansion.

ReB_2 was synthesized under ambient conditions via three methods, each of which may potentially be scaled up (supporting online text). First, a solid-state metathesis reaction was carried out between the metal trichloride and MgB_2, because this process has been used to produce many transition-metal diborides, including OsB_2 (*4*, *21*). Without excess B, however, this process forms multiple boride phases. Second, Re and B powders were mixed together, pressed into a pellet, and then liquefied with 80 amps of current in an Ar atmosphere. The result was a solid metallic ingot of ReB_2 that could be used for hardness testing. In the third method, stoichiometric quantities of Re and B powder were sealed in a quartz tube under vacuum and heated for 5 days at 1000°C. Powder x-ray diffraction, performed on a crushed portion of both the arc-melted ingot and the polycrystalline powder produced from the elements, confirmed the synthesis of phase-pure ReB_2 (fig. S1). These materials were then examined by microindentation and in situ high-pressure x-ray diffraction techniques.

To determine the Vickers hardness (H_V) of ReB_2, microindentation experiments were performed using a square pyramidal-shaped diamond indenter tip lowered onto a polished ingot with a known amount of force. When the indenter was removed, the area of the indent, indicating the extent of the plastic deformation of the sample, was measured. From this area and the applied load *P*, H_V was determined using Eq. 1

$$H_V = 1854.4\ P/d^2 \qquad (1)$$

where *d* is the arithmetic mean of the two diagonals of the indent.

Five indentations were made at varying loads on each of 10 grains of ReB_2. As the load was decreased from 4.9 to 0.49 N, the average hardness increased from 30.1 ± 1.3 to 48.0 ± 5.6 GPa, with a maximum measured hardness of 55.5 GPa under 0.49 N of load (Fig. 2A), which is comparable to the hardness of cubic BN under an equivalent load (*2*). The observed inverse relationship of applied load to hardness has been extensively documented in many different types of materials. This phenomenon is referred to as the indentation size effect. Although many factors may contribute to this effect, it is most frequently attributed to strain gradient plasticity in microindentation experiments (*22*). The superhard nature of ReB_2 was corroborated by a scratch test in which a piece of ReB_2 ingot was used to scratch a polished face of natural diamond parallel to the (100) plane (Fig. 2B).

The covalent bonding that results in high hardness values can also contribute to the elastic incompressibility (bulk modulus) of a material. To further explore the contribution of covalent bonding as well as the possible correlation between valence-electron density and bulk elastic

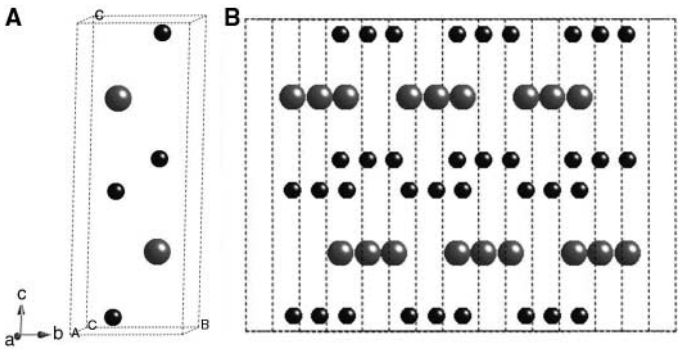

Fig. 1. The small dark spheres represent B atoms and the large light spheres represent Re. The structure is hexagonal with a = 2.9 Å and c = 7.478 Å. (**A**) A single unit cell. (**B**) Multiple unit cells demonstrating the layered structure viewed perpendicular to the $(3\bar{1}0)$ plane of ReB_2.

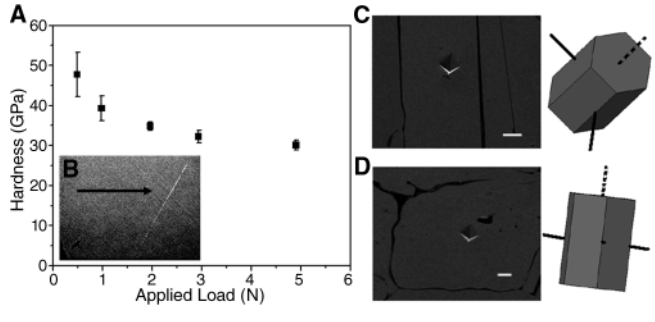

Fig. 2. (**A**) H_V of ReB_2 plotted as a function of applied load measured at room temperature, using a four-sided pyramidal diamond indenter tip. The average hardness increases from 30 to 48 GPa as the applied load decreases from 4.9 to 0.49 N (error bars = ±1SD). (**B**) An ingot of ReB_2 creates a scratch on the surface of a natural diamond parallel to the (100) plane. (**C**) Scanning electron microscope image of a diamond indentation under an applied load of 4.9 N in a ReB_2 grain yields a measured hardness of 31 GPa. The three-dimensional graphic at right corresponds to the crystallographic orientation of the indented grain. The dashed line is the *c* axis, and the solid lines lie parallel to the *a* and *b* directions. (**D**) Indentation on a grain with an orientation different from that in Fig. 2C (see graphic at right) produces a hardness of 27 GPa, consistent with the anisotropy of the hexagonal crystal structure of ReB_2. Scale bar in (C) and (D), 15 μm.

Downloaded from www.sciencemag.org on June 11, 2007

properties, data on the elastic volume compressibility of ReB_2 were collected via in situ high-pressure x-ray diffraction studies. Samples were compressed quasi-hydrostatically up to 30 GPa in a diamond anvil cell, and in situ diffraction data were collected under pressure. From the diffraction data, the fractional volume at increasing pressures was calculated. Fitting the pressure/volume (P versus V/V_0) data with a third-order Birch-Murnaghan equation of state, the bulk modulus of ReB_2 was determined to be 360 GPa when B_o' (derivative of the zero-pressure bulk modulus with respect to pressure) was fixed at the canonical value of 4. This high bulk modulus is in agreement with our understanding of the correlation between valence-electron density and incompressibility (*4*, *6*).

In addition to bulk volume compressibility, the high-pressure diffraction data also revealed an anisotropy in the compressibility of the two different lattice directions of hexagonal ReB_2 (Fig. 3). As seen in Fig. 3, the *c* axis is substantially less compressible than the *a* axis, and this *c* axis value is very similar to the analogous linear compressibility of diamond. This anisotropy results from greater electron density, and therefore greater electronic repulsions, along the *c* axis.

We sought to further elucidate the mechanical anisotropy among the crystallographic planes in ReB_2 through high-pressure radial diffraction experiments (*23*). These experiments differ from the conventional isotropic diamond anvil cell experiments described above. Here the material, held in place by a Be gasket, is intentionally subjected to nonhydrostatic pressures in a diamond anvil cell. The sample stress state can be divided into hydrostatic and deviatoric components. Hydrostatic compression of the sample results in elastic volume compression following the material's $P(V)$ equation of state. The deviatoric component is more complex, resulting from a combination of the applied-stress state and the sample mechanical response. To understand these plastic deformations, we consider the stress state inside the pressure cell. The direction of maximum stress is along the loading axis of the diamond anvil cell (σ_1), and the minimum stress direction is assumed to be cylindrically symmetric in the plane of the gasket (σ_3). The difference between these two stresses is the differential stress, t, which, if high enough, is capable of producing plastic deformation. Such high t values can be defined by the von Mises yield criterion (Eq. 2)

$$t = \sigma_1 - \sigma_3 \leq 2\tau = \sigma_y \qquad (2)$$

where τ is the shear strength and σ_y is the yield strength (*23*). Therefore, an estimate of t, provides a lower-bound estimate of the material's σ_y.

The differential stress can be calculated from measurements of lattice strain in the maximum and minimum stress directions and from knowledge of the single-crystal elastic properties via linear elasticity (*24*, *25*). The absence of single-crystal elastic moduli data necessitates the application of isotropic lattice strain theory for the analysis of strength in ReB_2. In this approach, we apply the isotropic theory to each lattice plane individually. Although substantial differences in strength behavior among different lattice planes are an indication of elastic anisotropy, we find that for related systems, the full anisotropic analysis does not substantially change the conclusions that can be drawn from the data.

For isotropic materials, the differential stress can be calculated from the lattice strain data using Eqs. 3 and 4

$$t = 6G\langle(\varepsilon_{hydro} - \varepsilon_{90})\rangle \qquad (3)$$

$$\varepsilon_{hydro} = (2\varepsilon_{90} + \varepsilon_0)/3 \qquad (4)$$

where G is the aggregate shear modulus of the polycrystalline sample; ε_{hydro} is the hydrostatic strain; and ε_{90} and ε_0 are the strains at the minimum and maximum stress orientations, respectively. These strains, specific for each lattice plane, are determined directly from the positions of the peaks in the x-ray diffraction patterns.

The greater the difference in the strain between the minimum and maximum stress directions, the greater the material's ability to support the differential stress in that plane without plastic deformation. In this experiment, data were collected from 0 to 14 GPa (Fig. 4), where ReB_2 supports a lattice averaged differential stress of 6.4 to 12.9 GPa, the highest measured for any material at these pressures. Other superhard materials, such as cubic Si_3N_4, B_6O, and TiB_2, are able to support only between 5 and 10 GPa of differential stress at these pressures (*26*–*28*). The lattice plane anisotropy is determined by the elastic anisotropy and perhaps also plastic anisotropy. As seen in Fig. 4, the (110) plane of ReB_2 is the stiffest plane and is able to support a differential stress of 17 GPa at 14 GPa of pressure. In contrast, the (004) plane shows a substantially lower differential stress. The difference in each lattice plane's ability to support differential stress can be attributed to the layered crystal structure of ReB_2. The (004) plane, which is orthogonal to the *c* axis and therefore lies parallel to the layers of Re and B, is likely to be a slip plane and a location of stress release in the material at high pressures. Consequently, it is able to support less differential stress than the other planes studied. In contrast, the (110) plane, which is perpendicular to these slip planes, is able to support the largest differential stress. Finally, as expected, the (101) plane, which has a component both parallel and perpendicular to the *c* axis, has an intermediate value between the (110) and (004) planes.

Having observed that the different planes of ReB_2 are able to support varying amounts of stress in the conventional and radial geometry

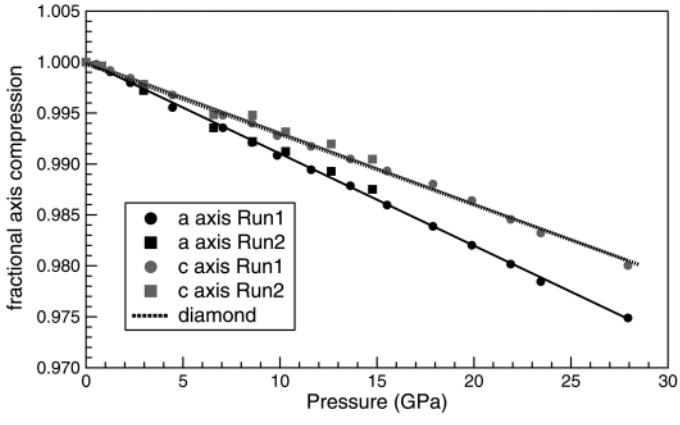

Fig. 3. There is substantial anisotropy in the compressibility of ReB_2. The *a* axis (black symbols) is more compressible than the *c* axis (gray symbols). The *c* axis of ReB_2 is as incompressible as the analogous axis of diamond (dashed line).

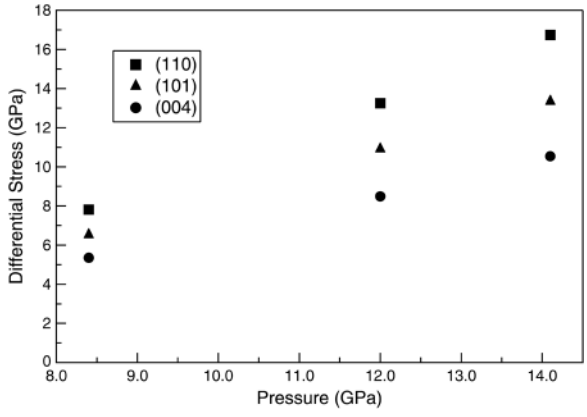

Fig. 4. When nonisotropic stress is applied to ReB_2, different planes support varying amounts of differential stress. The (110) plane (squares), which is orthogonal to the slip planes in ReB_2, exhibits the greatest ability to support differential stress, whereas the (004) plane (circles), which lies parallel to the slip planes, is able to support the least amount.

Downloaded from www.sciencemag.org on June 11, 2007

high-pressure experiments, we anticipated observing this effect in our hardness measurements as well. Indeed, Fig. 2A shows that there is a substantial difference between the highest and lowest measured hardness across grains of ReB_2 under the same load. This observed spread in hardness values at constant load can be attributed to the anisotropic structure of ReB_2, combined with our inability to control the crystallographic orientation of the tested grains. For example, under a load of 4.9 N, the highest measured hardness is 32.5 GPa and the lowest obtained value is 26.0 GPa.

We can begin to understand this variation in hardness by using electron backscattering diffraction to measure the orientations of the grains studied (Fig. 2, C and D). The results indicate that indentations parallel to the (00*l*) planes yielded the lowest average hardness, a value of 27 GPa. In contrast, indentations along directions that contained a larger component parallel to the *c* axis [that is, perpendicular to (00*l*)] resulted in measurements with an average hardness of 31 GPa, an increase of 15%. The dependence of hardness data on crystallographic orientation can be explained by the presence of the same slip planes described above. Furthermore, because similar anisotropic behavior is observed in the high-pressure data, we conclude that the radial diffraction study elucidates the plastic behavior of the material, giving an indication of the yield strength rather than merely measuring elastic behavior.

In our microindentation experiments to date, we have found no grains with pure (00*l*) orientation. As a result, our data demonstrate a minimum average hardness. It is likely that these planes parallel to (00*l*), which we were unable to directly measure, will have an even higher hardness and are responsible for scratching diamond (Fig. 2B).

References and Notes

1. P. F. McMillan, *Nat. Mater.* **1**, 19 (2002).
2. D. He *et al.*, *Appl. Phys. Lett.* **81**, 643 (2002).
3. V. L. Solozhenko, D. Andrault, G. Fiquet, M. Mezouar, D. C. Rubie, *Appl. Phys. Lett.* **78**, 1385 (2001).
4. R. W. Cumberland *et al.*, *J. Am. Chem. Soc.* **127**, 7264 (2005).
5. Incompressibility is the resistance to elastic volume compression and is reported as bulk modulus in units of gigapascals. Hardness is resistance to plastic deformation and is reported in units of force per unit area (in gigapascals).
6. R. B. Kaner, J. J. Gilman, S. H. Tolbert, *Science* **308**, 1268 (2005).
7. H. Cynn, J. E. Klepeis, C.-S. Yoo, D. A. Young, *Phys. Rev. Lett.* **88**, 135701 (2002).
8. F. Occelli *et al.*, *Phys. Rev. Lett.* **93**, 95502 (2004).
9. T. Kenichi, *Phys. Rev. B* **70**, 12101 (2004).
10. I. V. Aleksandrov, E. F. Goncharov, A. N. Zisman, S. M. Stishov, *Sov. Phys. JETP* **66**, 384 (1987).
11. H. J. McSkimin, W. L. Bond, *Phys. Rev.* **105**, 116 (1957).
12. M. H. Manghnani, K. Katahara, E. S. Fisher, *Phys. Rev. B* **9**, 1421 (1974).
13. C. A. Hampel, *Rare Metals Handbook* (Reinhold, London, 1961).
14. C. G. Fink, P. Deren, *Trans. Electro-chem. Soc.* **66**, 381 (1934).
15. A. Vegas, L. A. Martinez-Cruz, A. Ramos-Gallardo, A. Romero, *Z. Kristallogr.* **210**, 574 (1995).
16. S. La Placa, B. Post, *Acta Crystallogr.* **15**, 97 (1962).
17. Y. Z. Chen, H. J. Xiang, J. Yang, J. G. Hou, Q. Zhu, *Phys. Rev. B* **74**, 12102 (2006).
18. M. Hebbache, L. Stuparevic, D. Zivkovic, *Solid State Commun.* **139**, 227 (2006).
19. S. Chiodo, H. J. Gotsis, N. Russo, E. Sicilia, *Chem. Phys. Lett.* **425**, 311 (2006).
20. H. Gou *et al.*, *Appl. Phys. Lett.* **88**, 221904 (2006).
21. L. Rao, E. G. Gillan, R. B. Kaner, *J. Mater. Res.* **10**, 353 (1995).
22. H. Gao, Y. Huang, W. D. Nix, *Naturwissenschaften* **86**, 507 (1999).
23. A. L. Ruoff, *J. Appl. Phys.* **46**, 1389 (1975).
24. A. K. Singh, *J. Appl. Phys.* **73**, 4278 (1993).
25. A. K. Singh, C. Balasingh, H. K. Mao, R. J. Hemley, J. F. Shu, *J. Appl. Phys.* **83**, 7567 (1998).
26. B. Kiefer, S. R. Shieh, T. S. Duffy, T. Sekine, *Phys. Rev. B* **72**, 14102 (2005).
27. D. He, S. R. Shieh, T. S. Duffy, *Phys. Rev. B* **70**, 184121 (2004).
28. G. M. Amulele, M. H. Manghnani, M. J. Somayazulu, *J. Appl. Phys.* **99**, 23522 (2006).

29. This work was funded by NSF under grants DMR-0453121 (R.B.K.), EAR-0510914 (A.K.), and CMS-0307322 (S.H.T.), and an Integrative Graduate Education and Research Traineeship (J.B.L.). Use of the National Synchrotron Light Source, Brookhaven National Laboratory, and the Advanced Light Source, Lawrence Berkeley National Laboratory, were supported by the U.S. Department of Energy, Office of Basic Energy Science, under contracts DE-AC02-98CH10886 and DE-AC03-76SF00098, respectively. The authors thank S. Caldwell, S. Clark, R. Cumberland, S. Fakra, J. Gilman, J. Hu, M. Kunz, and A. Phan for their assistance with this research.

Supporting Online Material

www.sciencemag.org/cgi/content/full/316/5823/436/DC1
Materials and Methods
Fig. S1

26 December 2006; accepted 16 March 2007
10.1126/science.1139322

Facile Splitting of Hydrogen and Ammonia by Nucleophilic Activation at a Single Carbon Center

Guido D. Frey, Vincent Lavallo, Bruno Donnadieu, Wolfgang W. Schoeller,* Guy Bertrand*

In possessing a lone pair of electrons and an accessible vacant orbital, singlet carbenes resemble transition metal centers and thus could potentially mimic their chemical behavior. Although singlet di(amino)carbenes are inert toward dihydrogen, it is shown that more nucleophilic and electrophilic (alkyl)(amino)carbenes can activate H_2 under mild conditions, a reaction that has long been known for transition metals. However, in contrast to transition metals that act as electrophiles toward dihydrogen, these carbenes primarily behave as nucleophiles, creating a hydride-like hydrogen, which then attacks the positively polarized carbon center. This nucleophilic behavior allows these carbenes to activate NH_3 as well, a difficult task for transition metals because of the formation of Lewis acid-base adducts.

The activation of enthalpically strong small molecules such as molecular hydrogen (H_2) and ammonia (NH_3) has attracted considerable interest over the years. The first observation of H_2 splitting dates from the end of the 19th century, when Sabatier observed the formation of ethane in the addition of H_2 to ethylene over thin slivers of lightly heated reduced nickel (*1*). Since that time, most of the chemical and biological systems that have been found to split H_2 involve a transition metal center. Even for the so-called iron-sulfur cluster-free hydrogenase (Hmd), it has recently been shown that an iron center was of functional importance (*2*, *3*). The only nonmetallic systems reported to cleave H_2 under mild experimental conditions (*4*–*7*) are phosphine-borane species (*8*, *9*) and a stable digermyne (*10*).

In contrast to dihydrogen, ammonia usually forms simple Lewis acid-base adducts with transition metal complexes, as observed first by Werner in the late 19th century, because of the presence of a lone pair of electrons at nitrogen (*11*). Consequently, examples of NH_3 splitting are still very rare (*12*–*17*).

The activation of H-X and particularly H-H bonds requires that the pair of bonding electrons be perturbed in some way so as to form a chemically active species. The digermyne has substantial diradical character and therefore reacts through H atom abstraction from H_2, followed by recombination of the resultant radical pair (*10*). In contrast, the splitting of H_2 at a transition metal center results from the primary interaction of a vacant orbital at the metal and the σ-bonding orbital of H_2 (*18*–*22*) (Fig. 1). When concomitant back-donation from a filled *d* orbital to the anti-bonding σ* orbital of the bound H_2 is sufficiently strong, homolytic bond cleavage occurs. Otherwise, the acidic η^2-H_2 ligand undergoes proton transfer to another

UCR-CNRS Joint Research Chemistry Laboratory (UMI 2957), Department of Chemistry, University of California, Riverside, CA 92521–0403, USA.

*To whom correspondence should be addressed. E-mail: gbertran@mail.ucr.edu

Downloaded from www.sciencemag.org on June 11, 2007